Fabrication of inhaled hybrid silver/ciprofloxacin nanoparticles with synergetic effect against Pseudomonas aeruginosa

Article

Accepted Version

It is advisable to refer to the publisher's version if you intend to cite from the work. See Guidance on citing.

To link to this article DOI: http://dx.doi.org/10.1016/j.ejpb.2018.04.006

Publisher: Elsevier

www.reading.ac.uk/centaur

CentAUR

Central Archive at the University of Reading

Reading's research outputs online

Accepted Manuscript

Fabrication of inhaled hybrid silver/ciprofloxacin nanoparticles with synergetic effect against Pseudomonas aeruginosa

Hisham Al-Obaidi, Rachith Kalgudi, Mohammed Gulrez Zariwala

Please cite this article as: H. Al-Obaidi, R. Kalgudi, M. Gulrez Zariwala, Fabrication of inhaled hybrid silver/ciprofloxacin nanoparticles with synergetic effect against Pseudomonas aeruginosa, *European Journal of Pharmaceutics and Biopharmaceutics* (2018), doi: https://doi.org/10.1016/j.ejpb.2018.04.006

Fabrication of inhaled hybrid silver/ciprofloxacin nanoparticles with synergetic effect against Pseudomonas aeruginosa

Hisham Al-Obaidi[1] , Rachith Kalgudi[2] and Mohammed Gulrez Zariwala[2]

[1]The School of Pharmacy, University of Reading, Reading RG6 6AD, UK

[2] Faculty of Science & Technology, University of Westminster

115 New Cavendish Street, London, W1W 6UW

List of abbreviations

Ag: Silver

CF: Cystic fibrosis

CFX: Ciproflocxacin

CS: Chitosan

DMA: Dimethylamine

EE%: Entrapment efficiency

MBEC: Minimum biofilm eradication concentration

MIC: Minimum inhibitory concentration

NPs: Nanoparticles

TEOS: Tetraethyl orthosilicate

TPP: Sodium tripolyphosphate

TSI: twin stage glass impinge

*Corresponding author:

h.al-obaidi@reading.ac.uk

Abstract

Ciprofloxacin (CFX) is a fluroquinolone antibiotic used as a first line treatment against infections caused by *Pseudomonas aeruginosa* and *Streptococcus pneumonia* that are commonly acquired by cystic fibrosis (CF) patients. However, no inhalation formulation is currently available for ciprofloxacin. Hybrid silica coated silver nanoparticles were prepared using Stöber reaction and the optimum ratio of chitosan and sodium tripolyphosphate was used to encapsulate CFX. Particle deposition was assessed *in vitro* using twin stage impinger while antimicrobial activity was evaluated based on the planktonic growth of *P. aeruginosa* as well as against *P. aeruginosa* sp biofilm formation. *In vitro* deposition results showed significant deposition in stage 2 using twin stage impinger (TSI) (~70%). Compared to CFX, the formed hybrid nanoparticles were 3-4 folds more effective against inhibiting growth and biofilm formation by *P. aeruginosa* PAO1 and *P. aeruginosa* NCTC 10662.

Introduction

Cystic fibrosis (CF) is a multisystem genetic disorder caused by a mutation in cystic fibrosis transmembrane conductance regulator (CFTR) gene located on chromosome 7. The mutated gene leads to a malfunctioning protein causing hypersecretion of thick mucus which is difficult to clear. Due to the impaired mucosal defences, recurrent infections caused by *Psuedomonas aeruginosa* leading to chronic pulmonary symptoms and deteriorating lung function in CF patients. Various antimicrobial agents are used to treat respiratory infections of which the most commonly used is oral ciprofloxacin. *Pseudomonas aeruginosa* is a Gram-negative pathogen responsible for causing a wide range of nosocomial infections, most notably in immunocompromised patients. The infection is particularly challenging to treat due to the emergence of extended-spectrum-β-lactamase strains of *P. aeruginosa*. Its ability to form a robust biofilm as part of the infection makes it chronic and difficult to treat. The difficulty arises due to the production of a self-secreted extracellular polymeric substances (EPS) that form a protective matrix around the bacterial cells [1, 2]. Therefore, the need for alternatives to antibiotic treatment for this pathogen is becoming more apparent.

Ciprofloxacin (CFX) is a broad spectrum second generation fluoroquinolone antibiotic used effectively against wide range of infections including *P. aeruginosa* and *Streptococcus pneumonia* [3]. The current delivery methods available for CFX are oral and intravenous infusion and no inhaled formulation is currently available. It is also worth mentioning that prolonged administration of CFX could lead to severe gastrointestinal disturbances and

arthropathy, therefore it is not recommended for use in young children. Pulmonary drug delivery in particular is seen as a non-invasive approach as the lungs provide a thin, yet extremely efficient absorptive mucosal membrane with a good blood supply [4]. It is however challenging to deliver drugs to the highly viscous environment typically found in CF patients.

In order to overcome such limitations, the study of metal nanoparticles (NPs), functional core-shell colloidal NPs in particular, have gained extensive attention [5]. It is a well-known fact that silver (Ag) has strong antimicrobial properties and is still being used to treat wound infections [6]. Recently, silver nanoparticles have been found to increase bactericidal activity against *Staphylococcus aureus* in human osteoclasts [7].

Silver has also been found to have mucolytic properties combined with limited toxicity (based on suggested concentrations) in mammalian cells [8]. However, silver NPs may aggregate, coating with a silica shell is therefore essential to avoid loss of activity. Another issue has been the dissolution of silver when ammonia was used as a catalyst; hence this was replaced with dimethylamine whereby optimum coating could be achieved [9].

CFX is sparingly soluble in water, which may increase the chance for mucociliary clearance in the lungs; hence, the presence of silica may also aid the dissolution of CFX, which could minimize clearance. Nanoparticles encapsulating CFX and silver can be a promising solution to deliver the drug to the lungs to retain sufficient drug concentration above the minimum

inhibitory concentration (MIC). A broad variety of materials ranging from natural to synthetic have been used with a particular interest in polysaccharides such as chitosan (CS), a linear cationic polymer mainly degraded by lysozymes in the lungs [10]. Its cationic nature dictates its mucoadhesive properties as a result of electrostatic forces between the cationic amino groups of chitosan and the negatively charged glycoprotein of mucin [11]. This will provide a capacity allowing the entrapment of CFX, which will ensure effective delivery, and maintaining the drug at the target tissue.

The aim of this study was to prepare hybrid nanoparticles of silica coated silver nanoparticles embedded into a matrix of chitosan doped with ciprofloxacin. Secondly, to fully characterise the prepared nanoparticles and determine deposition efficiency using *in vitro* assessment followed by evaluating the antimicrobial activity in the main bacteria present in CF patients (*P. aeruginosa* PAO1 and *P. aeruginosa* NCTC 10662). This novel engineering of these nanoparticles has not been attempted before and it would therefore be very interesting to explore possible applications including delivery to the lungs.

Materials and methods

Materials

Tetraethyl orthosilicate (TEOS; ≥99.0%, GC, Aldrich), silver (Ag; nanopowder, <100 nm particle size, contains PVP as dispersant, 99.5% trace metals basis, Aldrich), chitosan (CS; low molecular weight, Aldrich), sodium tripolyphosphate (TPP; parum p.a., ≥98.0%, Sigma-Aldrich), ciprofloxacin (CFX; ≥98.0%, HPLC, Fluka), anhydrous lactose (Fluka), dimethylamine solution (DMA; 40 wt. % in H2O, Aldrich) and acetic acid (ReagentPlus®, ≥99%, Sigma-Aldrich) were obtained from Sigma-Aldrich, Dorset, UK. Ethanol absolute (EtOH) was obtained from VWR International, Leicestershire, UK.

Methods

Preparation of silica coated Ag and entrapment within chitosan-CFX matrix

75 mL of EtOH, 20 mL distilled water and silver nanoparticles were mixed followed by addition of 1 mL DMA combined with ultra sonication. Then to each of the flasks, 0.25, 0.5, 0.75 and 1 mL TEOS were added gradually whilst on vigorous stirring using mechanical stirrer. This created four suspensions containing different amounts of TEOS. The amount of Ag was also varied to allow comparison (2, 5, 7.5 and 10mg).

Determining the optimum ratio of CS:TPP

Prior to optimising the NPs, the loading efficiency of CS nanoparticles with CFX had to be determined and as indicated by a previous study [12]. CS:TPP of variable ratios ranging from 0.6 to 12.0 were tested using 0.3% w/v CS in 0.2% v/v acetic acid, 0.8% w/v CFX in 0.2% v/v acetic acid and 2% w/v TPP in water, note that all solutions were freshly made before mixing. The controlled variable was the amount of CFX and the independent variables were the amounts of CS and TPP used.

Formation of hybrid silica coated silver embedded in CS/CFX

CFX (120mg) was added to CS solution with 400 µL acetic acid while stirred vigorously to ensure complete dissolution. The suspension of the formed silica coated silver nanoparticles was then added to the CFX/CS solution and the mixture was kept stirring followed by drop wise addition of TPP which allows cross-linking of the CS. The formed suspensions were then spray dried using B-290 Buchi spray dryer using inlet temperature of 130 °C and an outlet temperature of 60°C. The resulting solid particles had silver content in the range of 0.047 to 0.14% w/w.

Particle size measurements using photon correlation spectroscopy and dissolution rate analysis

The formed nanoparticles were suspended in deionised water using different volumes (2 mL, 1 mL and 0.5 mL) and diluted using different dilution factors 10, 20 and 40 times respectively. Using photon correlation spectroscopy

(ZetaPlus, Brookhaven Instruments Corporation, USA), the count rate of the suspended particles was used as a measure of dissolution. These measurements were performed by withdrawing samples at different time intervals (0, 1, 3 and 5 hours) followed by dilution with water; all measurements are average of 10 replicates.

Transmission and scanning electron microscopy (TEM)

Selected samples were run under TEM to determine the size of the nanoparticles using Philips Tecnai T20 microscope operating at 200 kV equipped with an EDS (energy dispersive spectrum) detector.

X-ray powder diffraction

The polymorphic nature of the formed samples was studies using x-ray powder diffraction (XRPD). All samples were scanned using a Bruker D8 advance X-ray diffractometer (Bruker AXS GmbH, Germany) which is a Cu-source, theta– theta diffractometer equipped with a Lynx eye position sensitive detector. It was operated at 40 kV generator voltage and 40 mA generator current. The samples were analysed using DFFRAC plus XRD commander software (Bruker AXS GmbH, Germany) with a 2θ range of 5-45°, a step size of 0.02°and time per step of 1.33s.

In vitro equivalence testing using twin stage glass impinger (TSI)

Lactose was used as a carrier as because of its common use in dry powder inhalers where selected samples were mixed with lactose 5 minutes with the aim to generate uniform formulations. Three gelatine capsules containing 40 mg of each of the powder were filled for *in vitro* testing using TSI. About 7 mL and 30 mL of 0.2% v/v acetic acid were introduced in stages 1 and 2 respectively. Particle deposition was assessed *in vitro* using twin stage impinge using Rotahaler device and based on peak flow of 50L/min. The capsule under test was placed in the DPI followed by attachment to the mouthpiece and the fractions of deposition were measured by collecting the powders of mouthpiece and upper chamber (stage 1) and lower chamber (stage 2). The concentration was measured at λ271nm and the % CFX deposition in each stage was calculated accordingly as % ratio = deposited amount/ total emitted dose.

Bacterial strain, media and hybrid nanoparticles stocks

Pseudomonas aeruginosa PAO1 (wild type) and *P. aeruginosa* NCTC 10662 were obtained from The University of Westminster (London, UK) culture collection. The bacterial strains were cultured at 37° C for all experiments. Cation-adjusted Mueller–Hinton (CAMHB, Sigma-Aldrich, Dorset, UK) was used to determine minimum inhibitory concentrations (MICs) and minimal biofilm eradication concentration (MBEC). Luria-Bertani broth and agar (LBB and LBA, Sigma-Aldrich, Dorset, UK) was used for the determination of colony count for biofilm cell viability assay. Stock solutions of the hybrid

nanoparticle formulations were suspended in 0.1M acetic acid (Sigma-Aldrich, Dorset, UK). The stock solution was then used diluted in CAMHB to obtain desired concentrations.

Determination of Minimum inhibitory concentrations and MBEC

MIC values of the hybrid nanoparticles against *P. aeruginosa* PAO1 and *P. aeruginosa* NCTC 10662 were determined by broth dilution method and the obtained results were interpreted according to guidelines set by European Committee on Antimicrobial Susceptibility Testing, EUCAST guidelines [13]. Minimal biofilm eradication concentration (MBEC) of the formulations was determined by the method described by Rudilla *et al*., 2016 with a few modifications [14]. Briefly, pegs of a modified polystyrene lid (Nunc Immuno TSP system; catalog No. 445497) were immersed into separate 96-well microtiter plates containing 200 μL of LBB inoculated with *P. aeruginosa* PAO1 and *P. aeruginosa* NCTC 10662 per well, respectively. The plates were then incubated at 37 °C for a period of 24 h under static conditions. The pegs were gently rinsed twice during the process of MBEC determination with 0.5M PBS solution. The first wash effectively cleared the unattached planktonic cells while leaving behind the biofilm which was then immersed into a fresh set of 96-well plates containing different concentrations of hybrid nanoparticles which was then incubated for 24 h at 37 °C. After the second wash with 0.5M PBS solution, the biofilms were extracted by sonication for a period of 10 min. The bacteria, thus recovered from the biofilm were used to determine the MBEC values by recording the optical density of each treatment

at 600 nm. The lowest concentration of the hybrid nanoparticles that prevented growth of bacterial cells extracted from the treated biofilm was used to determine the MBEC. All the experiments were performed in triplicates. This work explores the potential of an effective hybrid nanoparticle treatment against a well-known biofilm forming Gram-negative pathogen as an alternative to mainstream antibiotics therapy. Experiments have thus specifically focused on demonstrating the effect of the hybrid nanoparticles on P. aeruginosa biofilm formation, since individual MIC of Ag, CFX and combinations have been widely explored and published in literature previously [15, 16].

Microtiter plate assay for biofilm quantification

P. aeruginosa PAO1 and *P. aeruginosa* NCTC 10662 biofilm was formed on 96 well flat bottom polystyrene micro-titre plates in triplicates. Briefly, A 10 µl of cell suspension having an absorbance of 0.5 at 600 nm was inoculated in 190 µl of LBB medium in each well. The microtiter plate was incubated for 18 h at 37° C. After aspiration of planktonic cells biofilms were fixed with 99% methanol. Plates were washed twice with 0.5M PBS and air-dried. Then, 200 µl of crystal violet solution (0.1%) was added to all wells. After 5 minutes, the excess crystal violet was removed and plates were washed twice and air dried. Finally, the biofilm bound crystal violet was dissolved in 33% acetic acid. Biofilm growth was measured at O.D 570 nm using a micro plate reader (BMG SPECTROstar Nano).

Biofilm bacteria enumeration after MIC treatment

P. aeruginosa PAO1 and *P. aeruginosa* NCTC 10662 biofilm was formed on 96 well flat bottom polystyrene micro-titre plates in triplicates. Briefly, A 10 µl of cell suspension having an absorbance of 0.5 at λ600 nm was inoculated in 190 µl of LBB medium in each well. The microtiter plate was incubated for 4 h and 12 h at 37° C. After aspiration of planktonic cells, 200 µl of 0.5M PBS was added to each well and sonicated for 10 minutes. 100 µl of recovered cells were then plated on pre-prepared LBA plates and incubated overnight at 37 °C and colonies were counted the following day.

Results

The first step was to form silica coated silver nanoparticles using a modified Stöber method. The core silver nanoparticles had a diameter of about 10nm with strong tendency to aggregate when dispersed in water. Hence, coating silver with silica layers will help to form a stable colloidal dispersion and prevent aggregation. The Stöber reaction is based on the base catalysed hydrolysis of tetraethyl orthosilicate using dimethylamine as a catalyst.

(1) $\quad\quad\quad Si(OR)_4 + H_2O \rightarrow (OR)_3Si(OH) + ROH$

(2) $\quad\quad\quad (OR)_3Si(OH) + H_2O \rightarrow SiO_2 + 3ROH$
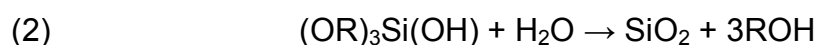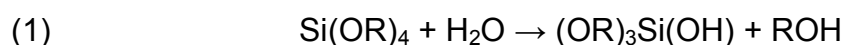
Different processes were subsequently performed so that the prepared hybrid particulates composed of chitosan matrix entrapping ciprofloxacin and encapsulating the silica coated silver nanoparticles.

Characterization of silica coated nanoparticles particles

Because of the possible dissolution of silver cores when ammonia is used as a catalyst, dimethylamine (DMA) was used to avoid such possible loss of the core [9]. In order to reach the best ratio of the core/shell, a factorial design of 36 formulations was prepared based on the independent variables used: Ag at 2, 5 and 7.5 mg, and TEOS at 1.1, 2.2, 3.4 and 4.5 mmol. As indicated above, The reaction is based on the hydrolysis of TEOS using alkaline conditions and ethanol as a solvent [17]. The formation of the nanoparticles was then assessed using size measurements (photon correlation spectroscopy and TEM) as well as turbidity measurements.

Photon correlation spectroscopy results showed a particle size range of 120-200nm for the silica coated silver nanoparticles (Figure 1). The results showed that increasing the amount of the core silver nanoparticles was associated with size increase signifying possible aggregation of the core silver nanoparticles. Broad variation was seen with the particles containing lower amount of TEOS (1.1 mmol) with narrower size distribution was observed

when the TEOS was increased. This may indicate better coating as the thickness of silica layers is increased.

Particle morphology and the particles' size distribution were further compared using TEM (Figure 2). The TEM images showed some variation whereby the particles that contained 4.5 mmol TEOS were more distinct and individualised. On the other hand, the particles containing 1.1 mmol TEOS were smaller in size and showed signs of aggregation with neighbouring particles which indicated the importance of isolating the cores and optimising the ratio of the silica coat. Encapsulation of silver nanoparticles was also evident as can be seen in the TEM images. The size however was slightly lower than the size obtained from PCS results with a size range of approximately 100-120nm. This variation in size was previously reported where dynamic light scattering measurements could deviate especially in the case of polydispersity [18].

Coating with chitosan layers with entrapped ciprofloxacin

As the optimum ratio of silica to core silver was determined, the next step was to embed the formed nanoparticles in chitosan matrix. Low molecular weight chitosan is a cationic polysaccharide synthesized by deacetylation of chitin. Its biodegradable, biocompatible and hydrophilic properties dictated its application in mucoadhesion and drug delivery [19]. In addition to hydrogen bonding potential with mucin, chitosan is polycationic hence can interact with the carboxyl and sulfate groups on mucin.

14

In order to enhance mucoadhesion properties of CFX containing NPs, it was important to ensure that the surface of the nanoparticles exhibits a positive charge. This was based on the Interaction between the cationic groups of CS with anionic regions of TPP. A range of weight ratios of CS to TPP was investigated to decide which ratio(s) was best for embedding the silver nanoparticles. The method is based on ionic gelation of the positive charge on chitosan with the oppositely charged TPP. Controlling the weight ratio is essential to ensure that complete bridging of the chitosan chains is achieved. Not reaching that level leads to poor formation of particles while excess amount of TPP can lead to inter-particle aggregation and agglomeration [12]. This was evident in Figure 3 where a significant aggregation of particles occurred at a weight ratio of chitosan/TPP 0.6-1.8. Beyond this ratio, consistent increase in particles size was observed where the size of the particles reached 1000nm. Zeta potential was measured for the formed particles within chitosan/TPP range of 4/1 to 2/1 and was 25-30 mv.

The last step was to embed the silver coated silica nanoparticles into the chitosan matrix. This also included encapsulation of CFX within the chitosan matrix. As CFX is soluble in acidic conditions, it was important to adjust the pH prior to forming the final particles. This was achieved via gradual change in the pH, using acetic acid to lower the pH to around 5-6. Based on the dissolution data, this pH was optimum to delay the dissolution of the silica layer. Based on obtained results, CFX was then loaded into particles that

were formed using chitosan/TPP ratio of 2 to 1 (pH was approximately 5.5). The formed particles were assessed visually and to examine whether these remain suspended or aggregate with time. Possible aggregation should be avoided as this can lead to lower entrapment of the drug and eventually poor delivery of the particles. Figure 2 shows the shape of the formed hybrid nanoparticles with a size range of 100-200 nm. The hollow matrix formed from chitosan can be seen entrapping the silica coated silver nanoparticles. The particles in Figure 2 showed agglomeration, as experimental conditions to perform SEM and TEM require the removal of the suspending liquid. The particles showed distinct spherical structures with no signs of aggregation, if agglomeration has happened; rough or irregular shaped particles would have been noticed. PCS analysis has been systematically performed for all particles (core nanoparticles), chitosan matrix and the final hybrid microparticles; overall, the size distribution was narrow and uniform.

The formed suspension of the final nanoparticles was spray dried to form solid particles. As can be been in Figure 2, the silica coated silver nanoparticles exhibited raspberry like structures with a size range similar to the size observed using TEM (liquid state prior to spray drying). Confirmation of the coating with silica and subsequent layers of chitosan was further confirmed using X-ray powder diffraction (Figure 4). The scans showed weakened intensity of silver diffraction peak as a result of coating with the silica and chitosan. The slight peak refers to the diffraction due to silver and the diminished peak is due to the amorphous silica coating, which reduced the intensity of the peak. These experiments were performed in conjunction with

16

SEM, TEM and PCS to demonstrate success and uniformity of coating. The appearance of slight peak could be due to two factors: coating with silica or lower silver content. However, the SEM and TEM images showed clear deposition of silica layers on silver cores hence we anticipate that the weakened X-ray peak is predominately because of the amorphous silica layers coating the silver nanoparticles.

Dissolution rate of hybrid nanoparticles

Dissolution rate was measured for particles using the count rate obtained from PCS because the size was considered as a controlling factor in the release of Ag and dissolution of CFX. The count rate is proportional to the size of the particles hence changes in count rate reflect changes in the size of the particles due to dissolution. Overall the results showed that the majority of the particles completely dissolved after 5 hours when dispersed in water. It is ideal to preserve the nanoparticles until they settle deep in the lungs and can then be engulfed by the bacteria. Premature dissolution leads to release of the drug with potential loss of activity.

By comparing the % dissolution (Figure 5) with the particle sizes, the results are more distinct in that it was not necessarily particles formed from lower TEOS that produced fastest dissolution rate. This is due to the fact that dissolution rate is influenced by particle aggregation whereby the surface area of the aggregated particles have substantially decreased. The amount of core

silver nanopartciles seemed to have variable impact on the dissolution of the particles where a change from 2 and 5 to 7mg resulted in a dissolution difference of up to 30%. Overall, the dissolution rates of measured samples could be described as fast with minimum impact of the core particles possibly signifying uniform coating. As shown in Figure 5, the dissolution of the particles was clear with the release of the silver nanoparticles supporting the dissolution results obtained using PCS measurements. The process started with the disintegration of the chitosan network followed by the release of silver, which could clearly be seen as the dark contrasted region. It was not clear whether the released silver nanoparticles aggregated and whether that was because of experimental conditions. Nevertheless, we expect that physiological conditions are more dynamic and release in situ would be more likely which helps to release the nanoparticles as individual entities. Typical physiological conditions involve diffusion of the alveolar fluid and airway epithelial cell cilia mobility. Overall, the formed silica nanoparticles were uniform as based on PCS measurements with very reproducible size range for different batches. The fate of the silica layers was demonstrated in Figure 5 where the size has decreased over time which demonstrates controlled release of the drug and core silver nanoparticles.

Measurement of deposition efficiency using TSI

The entrapment efficiency (EE%) of the formed hybrid nanoparticles was assessed after loading with CFX. The results showed that entrapment efficiency was highest for particles that were formed from chitosan/TPP 0.5 to

1 compared with other ratios (Table 1). Having showed EE% of approximately 73%, it was decided that the TSI measurements to be performed for samples using chitosan/TPP of 0.5 to 1. The details of samples that were run using TSI measurements are shown on Table 2.

As shown in Figure 6, significant fraction of the delivered particles was deposited in stage 2 with some formulations reaching 70% deposition. The deposition in this side represents the fine particle fraction (FPD%) which is vital for successful delivery of drugs deep inside the lungs. The emitted dose on the other hand varied among all formulations with the formulations that contained the lowest amount of silver cores being highest in terms of emitted dose (Figure 6). This could be attributed to the density differences where these are less dense, which may have affected the amount emitted from the device. While the formation of these particles has been a complex process, the outcome in terms of FPF was very promising.

Assessment of antimicrobial activity in *P. aeruginosa* biofilms

The final step was to assess whether the formed hybrid nanoparticles were more effective in terms of antibacterial activity compared with CFX alone. This was done using minimum inhibitory concentration as a measure of activity combined with inhibition of biofilm formation. The latter has been a problem as antibacterial resistance typically exists with *P. aeruginosa*

infections [20-22]. Stock concentrations of all the formulations were prepared in 0.1M acetic acid at 200 mcg/ml and diluted as and when required in the growth medium to obtain the required concentrations.

Cation-supplemented Mueller-Hinton broth was the medium used for identifying the MIC of Ciprofloxacin and other formulations. It allows good growth of most non-fastidious pathogens and is generally low in antagonists. Mueller-Hinton broth, which meets the requirements of the NCCLS standard, is considered the reference medium. The data presented in Table 3 show that the hybrid nanoparticles were highly effective against planktonic growth of P. aeruginosa PAO1 (wild type) and P. aeruginosa NCTC 10662 (commonly used control strain for antimicrobial sensitivity testing). Calgary Biofilm Device (CBD), a 96-well plate with pegs built into the lid that allows for the adherence and growth of biofilm was used. It is a highly efficient and accurate method of testing antimicrobial agent efficacy against biofilm formation. Compared to Ciprofloxacin, sample 2 and sample 3 were effective against inhibiting biofilm formation by P. aeruginosa PAO1 and P. aeruginosa NCTC 10662. Experiments were performed using Luria-Bertani broth and medium (Tables 3,4&5). This enhanced activity could clearly be seen Figure 7 where antimicrobial activity has increased approximately 3-4 times when hybrid nanoparticles were used. Overall, higher silver content resulted in greater antimicrobial activity. As shown in Tables 3,4&5, stock concentrations of all the formulations were prepared in 0.1M acetic acid at 200 mcg/ml of sample 2: 0.14% w/w Ag, 26.3% w/w CFX, 19.7% CS; Sample 3: 0.047% w/w Ag,

26.3% w/w CFX, 19.7% w/w CS, Sample 4: No silver, 30.7% w/w CFX, 23.1% w/w CS.

Discussion

Modified Stöber method based on using DMA rather than ammonia as the catalyst was successfully used to form silver core silica coated nanoparticles. Optimum ratio of chitosan was determined to form physically stable particles composed of chitosan as the matrix and contain silica coated silver nanoparticles. A ratio of CS:TPP of 0.5 to 1 seemed the best in terms of entrapment efficiency. The presence of an optimum ratio signifies the importance of ionic gelation in the formation of the final particles. This was reflected in the high entrapment efficiency where 73% of CFX was entrapped in the final particles.

The impact of silver in the shape, morphology and entrapment efficiency was critical. High loading with silver led to dense particles with possible separation and non-uniform mixing. This was avoided by varying the amounts of TEOS used so that to achieve a balance between silver content as well as optimum properties. Hence, the final TSI measurements were done using best ratios. Not surprisingly, particles with lowest silver content showed highest emitted dose. This however was balanced by the highest deposition of for most particles. Several studies have showed that the lung deposition might change in pulmonary diseases including cystic fibrosis (CF) due to alteration of the architecture and morphology of the lung in these conditions [3]. For

21

example, it has been reported previously that deposition was enhanced for fine and ultra-fine particles [23, 24]. Smaller sizes particles may thus facilitate better travel and penetration through the viscous mucous layer encountered in cystic fibrosis. We aim to develop this work further to perform in vivo studies to investigate whether the disease conditions will have significant impact on the delivery of the particles.

Assessment of the antibacterial activity revealed distinctive properties that correlated well with the silver content. At maximum loading with Ag, it was possible to achieve almost 3-4 times greater antimicrobial activity.   This enhanced activity can also be linked with the recent findings on the role of silver nanoparticles on the enhanced activity in human osteoclasts [7]. The authors showed that silver nanoparticles were non-toxic at concentrations below ~12μg which suggests that formed hybrid nanoparticles are non-toxic with enhanced antibacterial activity.   Stock concentrations of all the formulations were prepared in 0.1M acetic acid at 200 μg/ml and diluted as and when required in the growth medium to obtain the required concentrations. For MIC experiments stock of 200 μg/mL in acetic acid that was diluted several times to yield a final concentration 4 μg/mL while for biofilm experiments the final concentration of 5 ug/ml was used. This implies that the used silver amount is significantly below the stated safety level of 12μg. The FDA has categorized colloidal silver as an unclassified drug [25]. Silver is available as homeopathic remedy (as colloidal silver mist spray) despite potential side effects (argyria and bluish discoloration of the skin). However, the concentration used in this study is significantly small.   For

comparison, homeopathic preparations contain 10-40ppm, and the silver content used in this study was 4-5ppm. Nevertheless, it is difficult to anticipate potential hazards without further research on long-term effects, which will be the focus of our future research; the authors hope that these significantly low concentrations will have therapeutic applications while having negligible undesirable effects. Silica nanoparticles are used in cosmetic, food packaging and industrial applications. Their deposition and clearance mechanisms in the lungs are considered to be similar to conventional nanoparticles of identical size range. Several studies have investigated in vitro and in vivo cytotoxic effects and while issue of toxicity are known, it has been regarded that the toxicity is dose dependent as well as subject to the frequency of exposure. Studies also suggest that unmodified silica nanoparticles can potentially cause greater cytotoxic effects and ROS induction than surface modified ones [26]. The composite nature of the prepared hybrid nanoparticles might render silica less prone to causing cytotoxic and pro-oxidant effects. In order to confirm this, future research will include comprehensive studies of cytotoxicity, cellular uptake and ROS induction.

Conclusions

The work presented here shows for the first time that it is possible to use silver at sub-toxic levels to achieve 3-4 times greater antibacterial activity. Properties of the final particles were optimised so as to ensure maximum entrapment efficiency with maximum deposition deep inside the lungs. It was

possible to prepare hybrid nanoparticles with entrapment efficiency of approximately 73% with optimum deposition. A higher rate of biofilm inhibition was achieved with sub-toxic levels of hybrid nanoparticles when compared against two strains of *P. aeruginosa* after a treatment period of 12 h under in vitro conditions. Enumeration bacterial cells extracted from the biofilm after 12 h treatment showed a significant decrease in cell count which equates to high level of bactericidal activity against biofilm forming sessile cells. This shows us that the hybrid nanoparticles used in this study are effective against sessile cells of CF causing pathogen, *P. aeruginosa* that are protected by the EPS layer and are hard to reach and target using conventional antibiotic therapy.

Acknowledgements

References

[1] W.A. El-Shouny, S.S. Ali, J. Sun, S.M. Samy, A. Ali, Drug resistance profile and molecular characterization of extended spectrum beta-lactamase (ESbetaL)-producing Pseudomonas aeruginosa isolated from burn wound infections. Essential oils and their potential for utilization, Microbial pathogenesis, 116 (2018) 301-312.

[2] S.V. van der Waal, J. de Almeida, B.P. Krom, J.J. de Soet, W. Crielaard, Diffusion of antimicrobials in multispecies biofilms evaluated in a new biofilm model, International endodontic journal, 50 (2017) 367-376.

[3] N.R. Labiris, M.B. Dolovich, Pulmonary drug delivery. Part I: physiological factors affecting therapeutic effectiveness of aerosolized medications, British journal of clinical pharmacology, 56 (2003) 588-599.

[4] P. Calvo, C. Remuñan-López, J.L. Vila-Jato, M.J. Alonso, Chitosan and Chitosan/Ethylene Oxide-Propylene Oxide Block Copolymer Nanoparticles as Novel Carriers for Proteins and Vaccines, Pharmaceut Res, 14 (1997) 1431-1436.

[5] V.R. Baral, A.L. Dewar, G.J. Connett, Colloidal silver for lung disease in cystic fibrosis, Journal of the Royal Society of Medicine, 101 Suppl 1 (2008) S51-52.

[6] M. Rai, A. Yadav, A. Gade, Silver nanoparticles as a new generation of antimicrobials, Biotechnology advances, 27 (2009) 76-83.

[7] V. Aurore, F. Caldana, M. Blanchard, S.K. Hess, N. Lannes, P.Y. Mantel, L. Filgueira, M. Walch, Silver-nanoparticles increase bactericidal activity and radical oxygen responses against bacterial pathogens in human osteoclasts, Nanomedicine, (2017).

[8] Q.L. Feng, J. Wu, G.Q. Chen, F.Z. Cui, T.N. Kim, J.O. Kim, A mechanistic study of the antibacterial effect of silver ions on Escherichia coli and Staphylococcus aureus, Journal of biomedical materials research, 52 (2000) 662-668.

[9] Y. Kobayashi, H. Katakami, E. Mine, D. Nagao, M. Konno, L.M. Liz-Marzan, Silica coating of silver nanoparticles using a modified Stober method, J Colloid Interface Sci, 283 (2005) 392-396.

[10] R.J. Nordtveit, K.M. Vårum, O. Smidsrød, Degradation of partially N-acetylated chitosans with hen egg white and human lysozyme, Carbohydrate polymers, 29 (1996) 163-167.

[11] R. Osman, P.L. Kan, G. Awad, N. Mortada, A.E. El-Shamy, O. Alpar, Spray dried inhalable ciprofloxacin powder with improved aerosolisation and antimicrobial activity, Int J Pharm, 449 (2013) 44-58.

[12] A. Rampino, M. Borgogna, P. Blasi, B. Bellich, A. Cesaro, Chitosan nanoparticles: preparation, size evolution and stability, Int J Pharm, 455 (2013) 219-228.

[13] C. Hasselmann, E.S.C. Microbiology, Determination of minimum inhibitory concentrations (MICs) of antibacterial agents by broth dilution, Clin Microbiol Infec, 9 (2003).

[14] H. Rudilla, E. Fuste, Y. Cajal, F. Rabanal, T. Vinuesa, M. Vinas, Synergistic Antipseudomonal Effects of Synthetic Peptide AMP38 and Carbapenems, Molecules, 21 (2016).

[15] K. Markowska, A.M. Grudniak, K. Krawczyk, I. Wróbel, K.I. Wolska, Modulation of antibiotic resistance and induction of a stress response in Pseudomonas aeruginosa by silver nanoparticles, Journal of Medical Microbiology, 63 (2014) 849-854.

[16] A. Grillon, F. Schramm, M. Kleinberg, F. Jehl, Comparative Activity of Ciprofloxacin, Levofloxacin and Moxifloxacin against Klebsiella pneumoniae, Pseudomonas aeruginosa and Stenotrophomonas maltophilia Assessed by Minimum Inhibitory Concentrations and Time-Kill Studies, PloS one, 11 (2016).

[17] H.P. Jarvie, H. Al-Obaidi, S.M. King, M.J. Bowes, M.J. Lawrence, A.F. Drake, M.A. Green, P.J. Dobson, Fate of silica nanoparticles in simulated primary wastewater treatment, Environ Sci Technol, 43 (2009) 8622-8628.

[18] Z.H. Chen, C. Kim, X.B. Zeng, S.H. Hwang, J. Jang, G. Ungar, Characterizing size and porosity of hollow nanoparticles: SAXS, SANS, TEM, DLS, and adsorption isotherms compared, Langmuir, 28 (2012) 15350-15361.

[19] M. Dash, F. Chiellini, R.M. Ottenbrite, E. Chiellini, Chitosan—A versatile semi-synthetic polymer in biomedical applications, Progress in Polymer Science, 36 (2011) 981-1014.

[20] T. Bjarnsholt, P.O. Jensen, M.J. Fiandaca, J. Pedersen, C.R. Hansen, C.B. Andersen, T. Pressler, M. Givskov, N. Hoiby, Pseudomonas aeruginosa Biofilms in the Respiratory Tract of Cystic Fibrosis Patients, Pediatr Pulm, 44 (2009) 547-558.

[21] N. Hoiby, O. Ciofu, T. Bjarnsholt, Pseudomonas aeruginosa biofilms in cystic fibrosis, Future Microbiol, 5 (2010) 1663-1674.

[22] N. Hoiby, H.K. Johansen, C. Moser, O. Ciofu, P.O. Jensen, M. Kolpen, L. Mandsberg, M. Givskov, S. Molin, T. Bjarnsholt, Pseudomonas aeruginosa Biofilms in the Lungs of Cystic Fibrosis Patients, Biofilm Infections, (2011) 167-184.

[23] R. Sturm, An advanced stochastic model for mucociliary particle clearance in cystic fibrosis lungs, Journal of thoracic disease, 4 (2012) 48-57.

[24] P. Brand, T. Meyer, S. Haussermann, M. Schulte, G. Scheuch, T. Bernhard, B. Sommerauer, N. Weber, M. Griese, Optimum peripheral drug deposition in patients with cystic fibrosis, Journal of aerosol medicine : the official journal of the International Society for Aerosols in Medicine, 18 (2005) 45-54.

[25] Over-the-counter drug products containing colloidal silver ingredients or silver salts. Department of Health and Human Services (HHS), Public Health Service (PHS), Food and Drug Administration (FDA). Final rule, Federal register, 64 (1999) 44653-44658.

[26] V. Marzaioli, J.A. Aguilar-Pimentel, I. Weichenmeier, G. Luxenhofer, M. Wiemann, R. Landsiedel, W. Wohlleben, S. Eiden, M. Mempel, H. Behrendt, C. Schmidt-Weber, J. Gutermuth, F. Alessandrini, Surface modifications of silica nanoparticles are crucial for their inert versus proinflammatory and immunomodulatory properties, International journal of nanomedicine, 9 (2014) 2815-2832.

Legend to Figures

Figure 1: Diameter of nanoparticles prepared using different ratios of TEOS and Ag.

Figure 2: (A) Transmission electron microscopy showing silica-coated silver nanoparticles with multiple silver nanoparticles were entrapped, (B) transmission electron microscopy showing the clusters formed from the silica coated silver nanoparticles entrapped within chitosan layers, (C) scanning electron microscopy showing "raspberry" structures formed form silica coated silver nanoparticles embedded particles in chitosan matrix and (D) scanning electron microscopy showing "raspberry" structures formed form silica coated silver nanoparticles.

Figure 3: The diameter of the chitosan nanoaprticles formed using different ratios of chitosan/TPP and as measured using dynamic light scattering

Figure 4: X-ray powder diffraction showing prepared particles, shaded bars indicate weakened intensity as the silver nanoparticles is coated with silica and chitosan.

Figure 5: Dissolution of the hybrid nanoparticles after exposure to aqueous media for 1,3 and 5 hours as measured using photon correlation spectroscopy for (A) NPs prepared using 2mg, (B) 5mg and (C) 7.5mg Ag. The dissolution was evident using transmission electron microscopy for the hybrid nanoparticles as shown in (D).

Figure 6: Assessment of the in vitro deposition represented as % deposition of CFX in stage 1 and 2 in TSI compared with the emitted (µg) dose from the device for different formulations.

Figure 7: Activity of Ciprofloxacin and formulations against *P. aeruginosa* sp biofilm formation after 18h of growth. Experiments performed in 96-well microtiter plates using ½ MIC of respective samples and compared against untreated control. Stock concentrations of all the formulations were prepared in 0.1M acetic acid at 200 mcg/ml of sample 2: 0.14% w/w Ag, 26.3% w/w CFX, 19.7% CS; Sample 3: 0.047% w/w Ag, 26.3% w/w CFX, 19.7% w/w CS, Sample 4: No silver, 30.7% w/w CFX, 23.1% w/w CS.

Legend to Tables

Table 1: The entrapment efficiency of CFX entrapped nanoparticles using different ratios of CS/TPP.

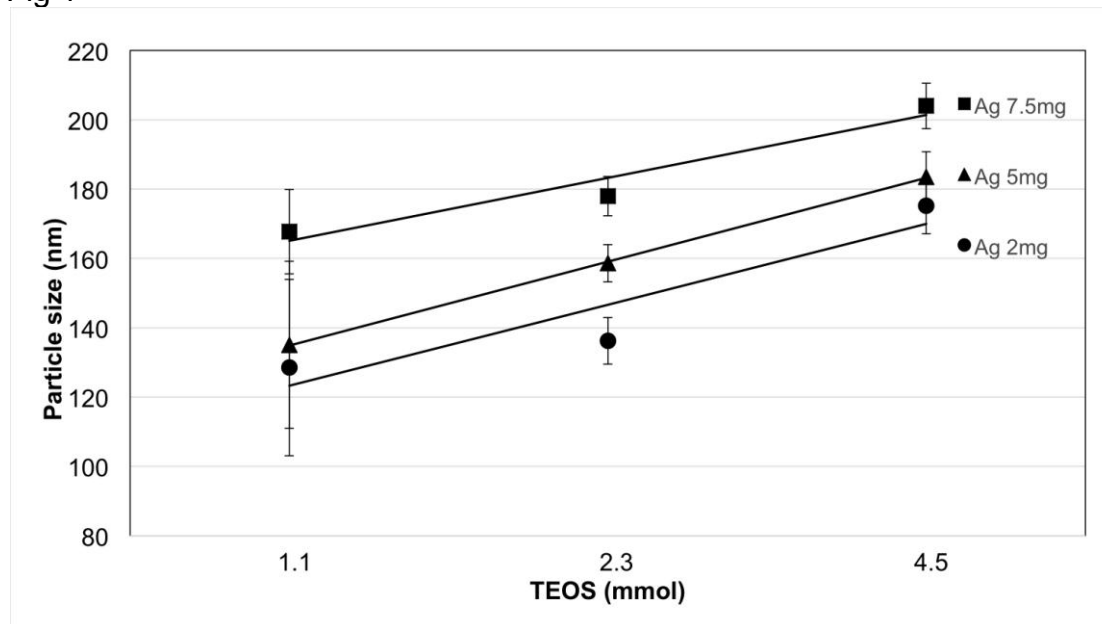**Table 2:** Composition of hybrid nanoparticles that were selected for TSI measurements

Table 3: Minimum inhibitory concentration (MIC) by broth dilution method.

Table 4: Minimum biofilm eradication concentration (MBEC) by broth dilution method.

Table 5: Biofilm cell enumeration (viability) by plating.

Fig 1

Fig 2

Fig 3

Fig 4

Fig 5

Fig 6

Fig 7

Effect of formulations on *P. aerugionsa* sp Biofilm formation
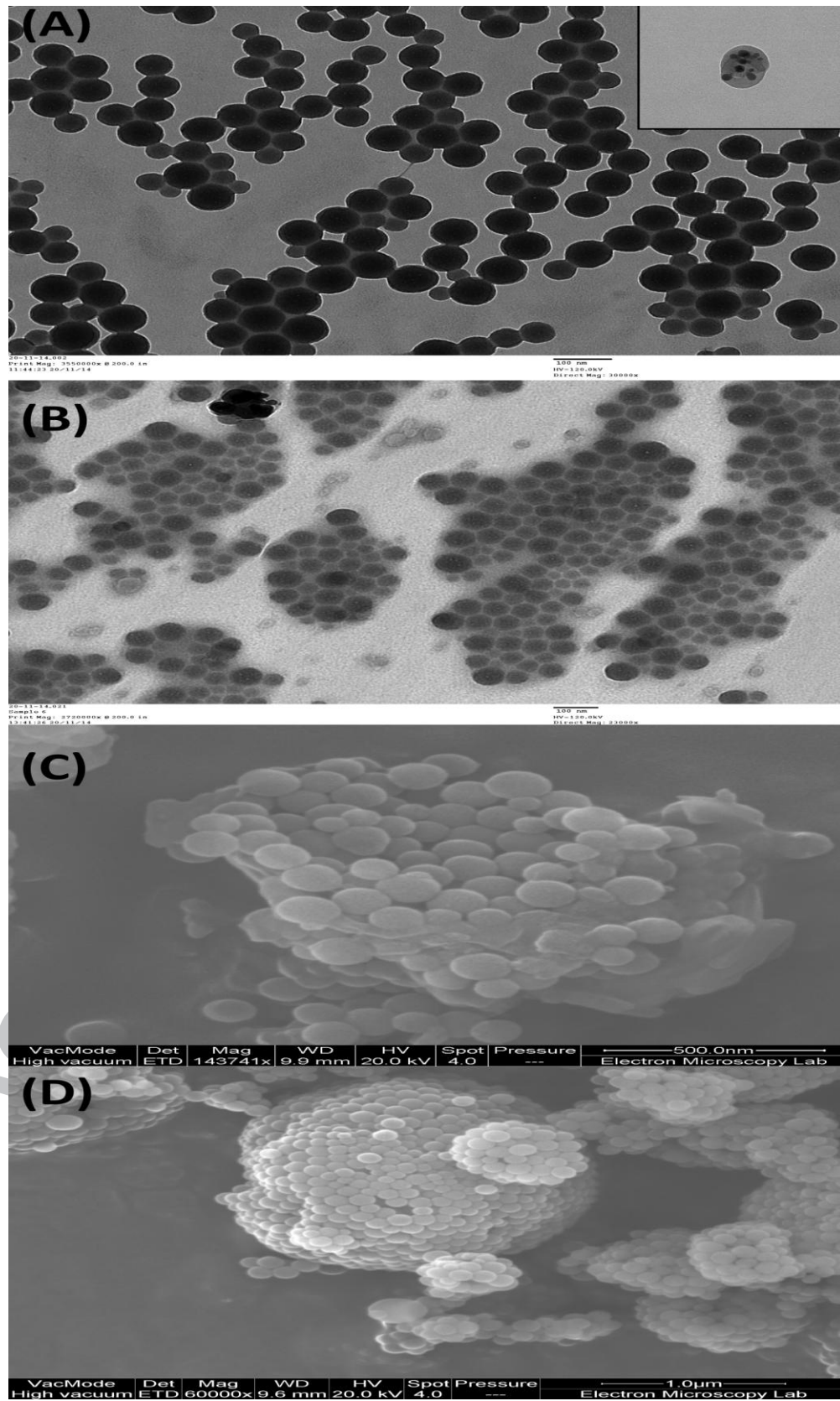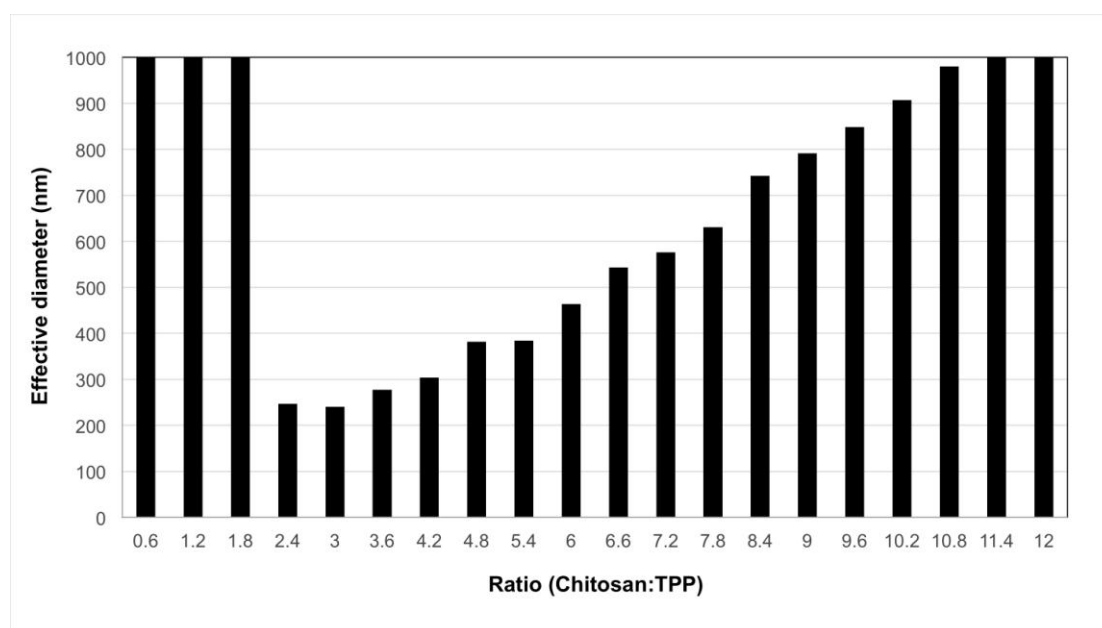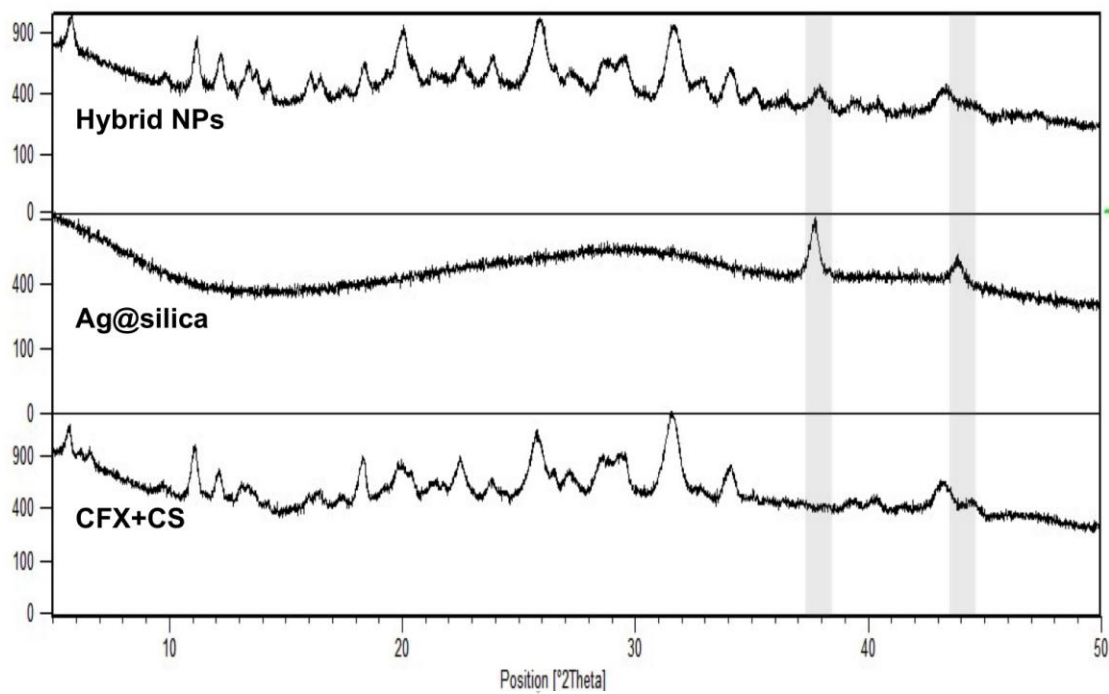
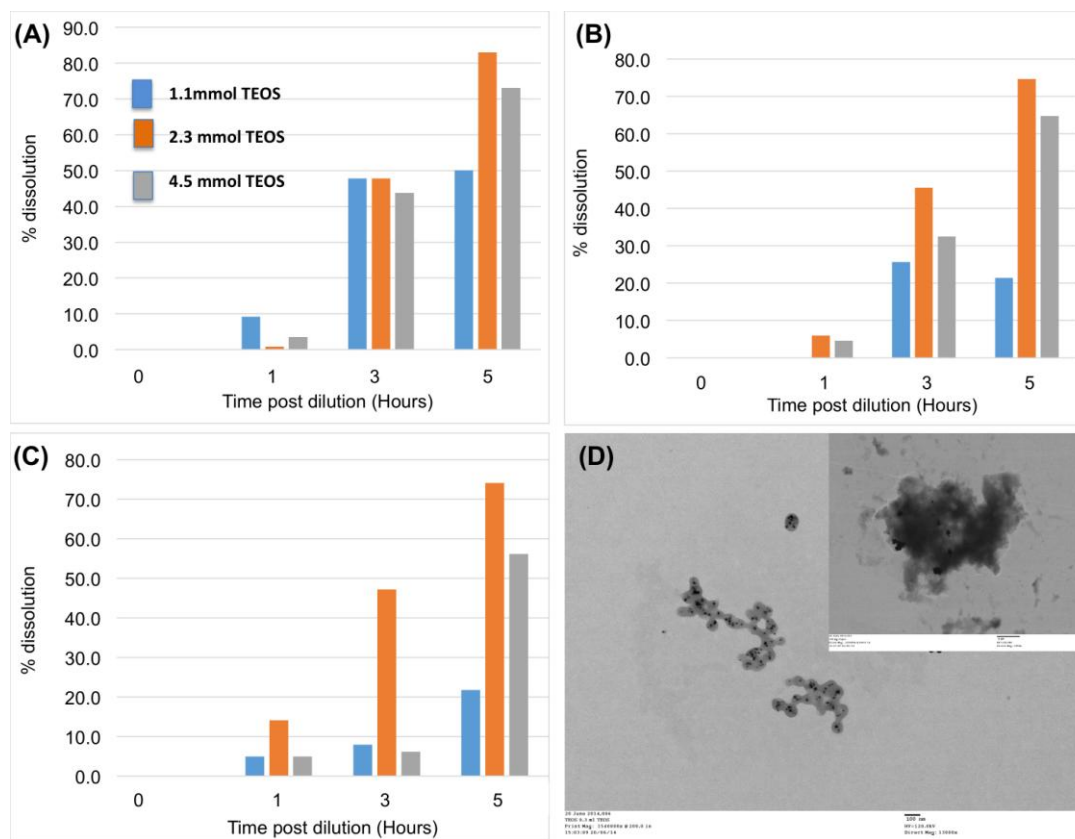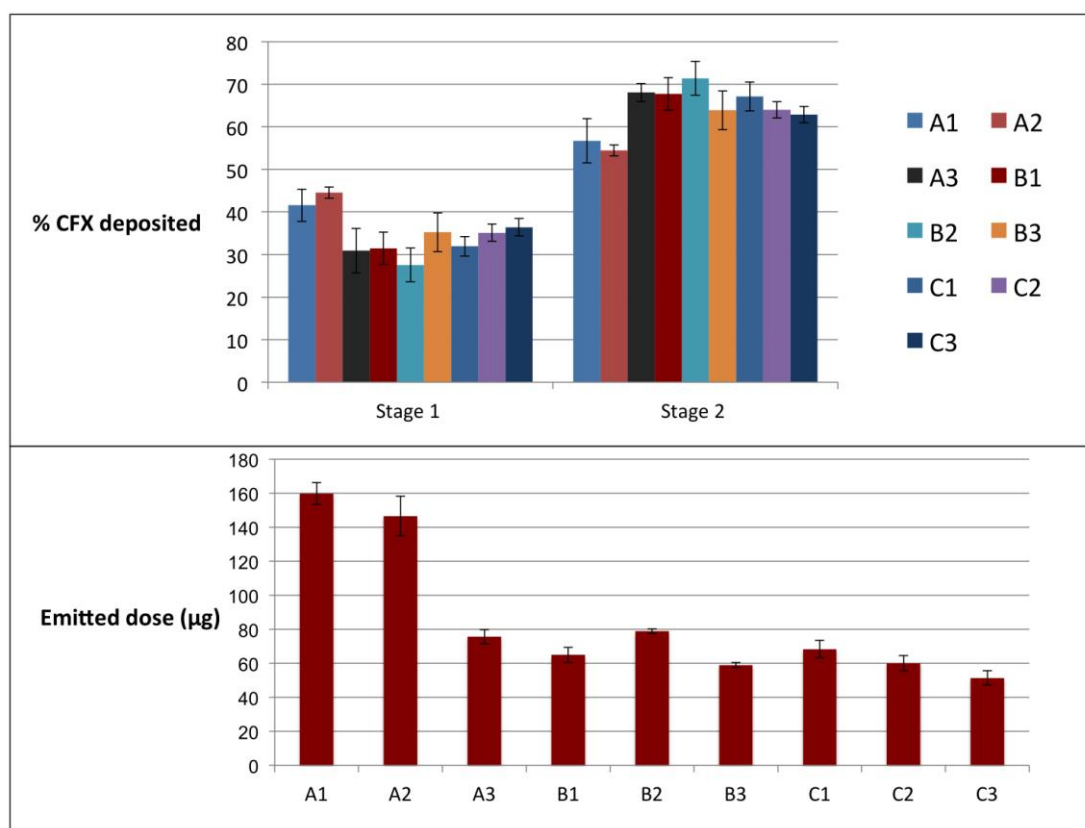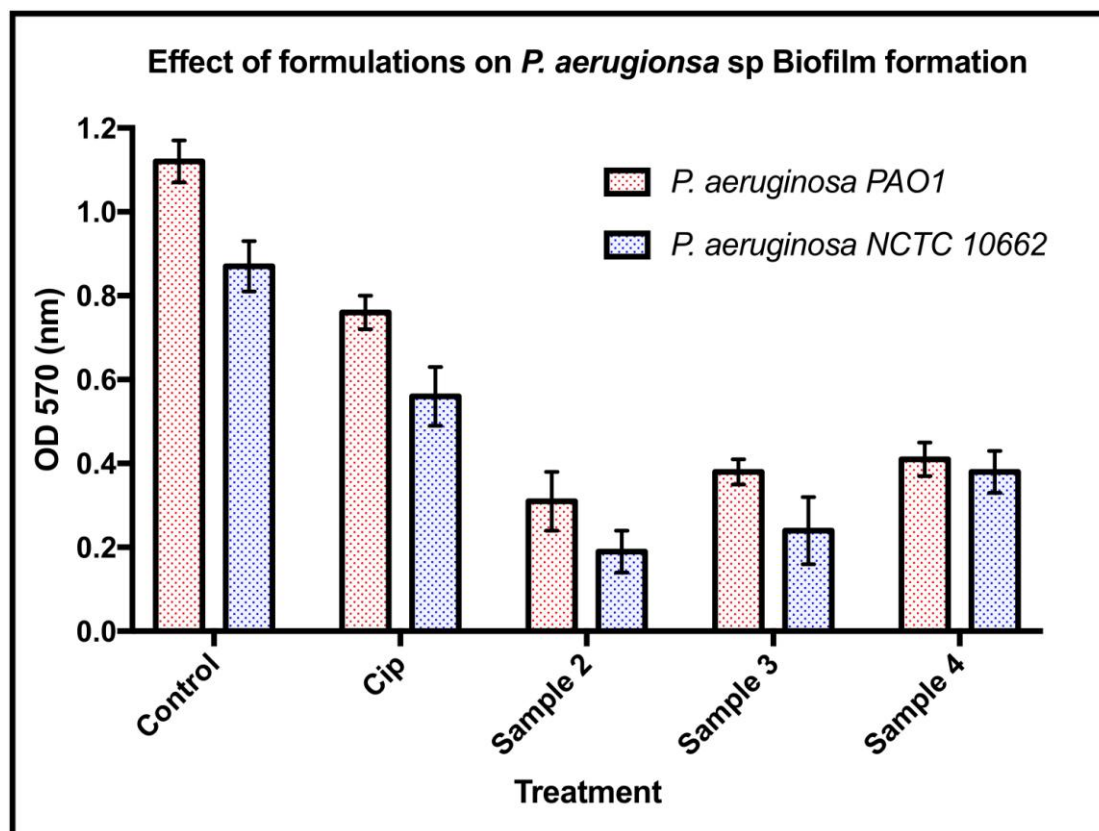**Table 1:** The entrapment efficiency of CFX entrapped nanoparticles using different ratios of CS/TPP.

Ratio (CS/TPP)	% EE ± sd
0.5	72.7 ± 0.8
1	38.0 ± 0.9
2	16.1 ± 1.8
3	10.2 ± 2.3
4	12.1 ± 1.1

Table 2: Composition of hybrid nanoparticles that were selected for TSI measurements

Formula code	Ag (mg)	TEOS (mL)	CS (mg)	TPP (mg)	CFX (mg)
A1	2.0	0.25	90	180	120
A2	2.0	0.50	90	180	120
A3	2.0	0.75	90	180	120
B1	5.0	0.25	90	180	120
B2	5.0	0.50	90	180	120
B3	5.0	0.75	90	180	120
C1	7.5	0.25	90	180	120
C2	7.5	0.50	90	180	120
C3	7.5	0.75	90	180	120

Table 3: Minimum inhibitory concentration (MIC) by broth dilution method.

Organism	Cip	Sample 2	Sample 3	Sample 4
	MIC µg/ml			
P. aeruginosa **PAO1**	24	8	12	16
P. aeruginosa **NCTC 10662**	16	4	8	12

Table 4: Minimum biofilm eradication concentration (MBEC) by broth dilution method.

Organism	Cip	Sample 2	Sample 3	Sample 4
	MBEC µg/ml			
P. aeruginosa **PAO1**	105	15	45	65
P. aeruginosa **NCTC 10662**	50	10	25	40

Table 5: Biofilm cell enumeration (viability) by plating.

Sample	Time	Organism	
		P. aeruginosa PAO1	*P. aeruginosa* NCTC 10662
		log10 cfu/ml	
CFX	4h	2.2 ± 0.24	1.02 ± 0.4
	12h	0.57 ± 0.53	0.15 ± 0.45
2	4h	1.41 ± 0.21	0.68 ± 0.35
	12h	0.21 ± 0.1	0.08 ± 0.21
3	4h	1.38 ± 0.16	0.79 ± 0.31
	12h	0.63 ± 0.12	0.07 ± 0.32
4	4h	1.93 ± 0.21	1.10 ± 0.12
	12h	1.21 ± 0.43	0.87 ± 0.35

± depicts standard deviation, n=3

Graphical abstract